

FR 8600 369

COMMISSARIAT A L'ENERGIE ATOMIQUE

CENTRE D'ETUDES NUCLEAIRES DE SACLAY

Service de Documentation

F91191 GIF SUR YVETTE CEDEX

CEA-CONF -- 8043

L3

Rapport DPh-N/Saclay n°2297

PION PHOTOPRODUCTION IN NUCLEI

Nico de Botton

Service de Physique Nucléaire - Haute Energie
CEN Saclay, 91191 Gif-sur-Yvette Cedex, France

Communication présentée à : 5.Course on intermediate energy nuclear physics
Verona (Italy)
20-30 Jun 1985

PION PHOTOPRODUCTION IN NUCLEI

Nico de Botton

Service de Physique Nucléaire - Haute Energie
CEA Saclay, 91191 Gif-sur-Yvette Cedex, France

ABSTRACT

We discuss pion photoproduction experiments in connection with experimental techniques used for the photon source and the pion detection. After presenting the physical motivations and the theoretical frame of interpretation, we report on a few significant experiments displaying different aspects of the field.

1. Introduction

A glance at fig. 1 will convince that pion photoproduction on a nucleus is the most important reaction channel in the photon energy region going from threshold up to 600 MeV. The data represented here come from a recent total absorption photon experiment on carbon performed at the

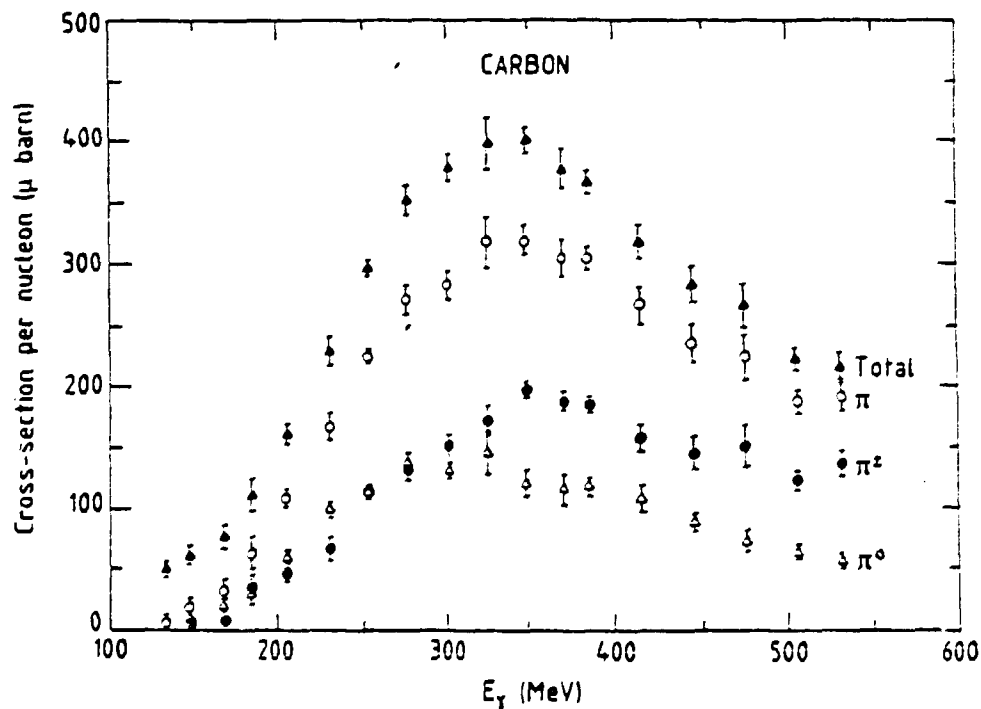


Fig. 1 - ^{12}C photonuclear total cross sections¹⁾: total absorption, pion production, charged pions and neutral pions.

Saclay linac¹). In this experiment which used a tagged annihilation photon beam, partial identification of the reaction channels was possible. The sum of charged and neutral pion cross sections is shown to account for more than 80 % of the total absorption cross section throughout the explored energy range. The remaining part of the cross section is mostly emission of neutron proton pairs ; it is also a manifestation of a pion photoproduction process in which the pion created on a nucleon has been subsequently absorbed on another nucleon correlated to the first one. Variation with energy of all cross sections shows clearly the dominance of the $\Delta(1232)$ resonance.

In fig. 2 we display a π^+ spectrum obtained using a quasi-monochromatic annihilation photon beam on a ^3He target²). The spectrum exhibits a broad peak corresponding to the quasi-free photoproduction process and a narrow line at the upper tip related to the elastic production process leaving the residual nucleus in the ^3H ground state.

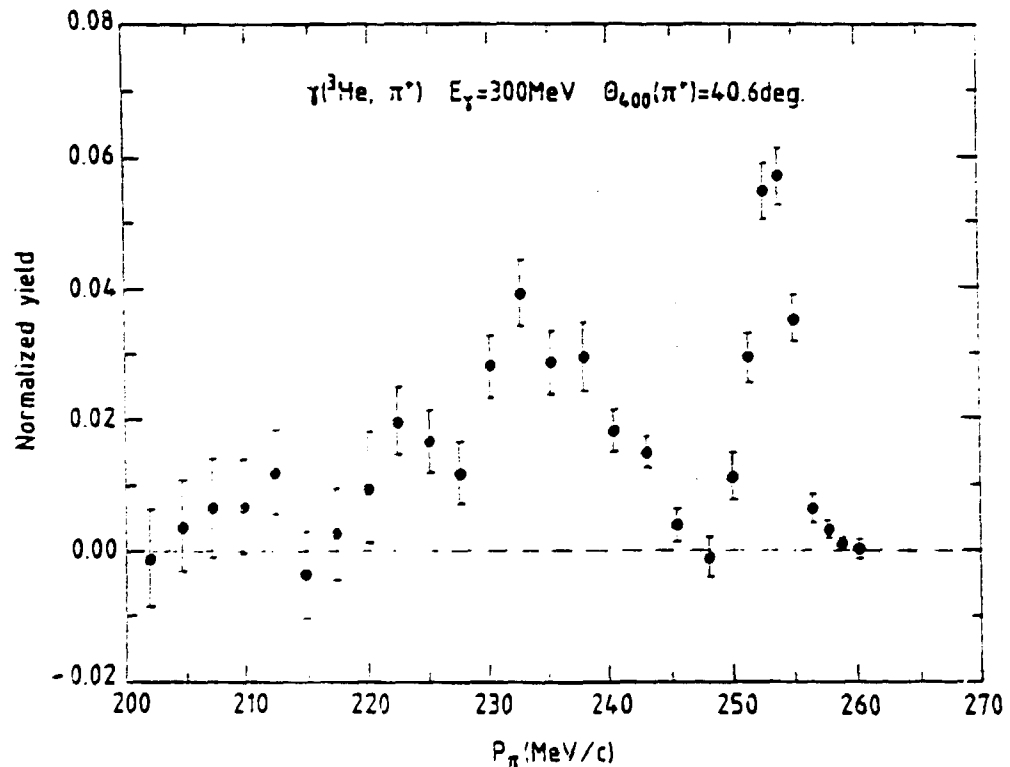


Fig. 2 - The momentum spectrum of π^+ photoproduction on ^3He at $E_\gamma = 300$ MeV and $\theta = 40.6^\circ$.

One is surprised to find out that there are very few such examples of inclusive data which give overall information on pion photoproduction on nuclei. Instead most of the work of these last years has been devoted to the study of very exclusive charged pion photoproduction reactions using continuous Bremsstrahlung photon spectra or equivalently virtual

photon spectra in single-arm electroproduction measurements. For instance, we see in fig. 3 the differential cross section of the reaction $^{28}\text{Si}(\gamma, \pi^+)^{28}\text{Al}$ measured at 179 MeV for a 2.2 MeV excitation of the ^{28}Al residual nucleus³⁾ corresponding to a strong M1 transition.

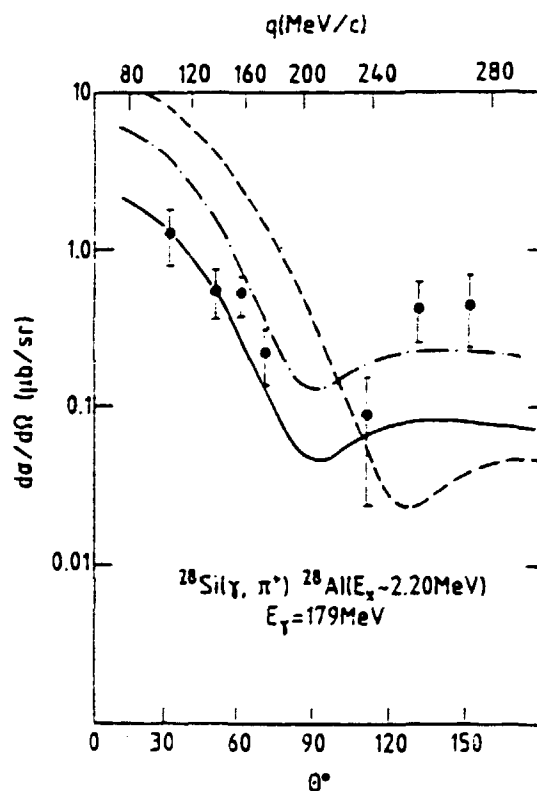


Fig. 3 - The angular distribution of π^+ in $^{28}\text{Si}(\gamma, \pi^+)^{28}\text{Al}$ ($E_x \sim 2.2$ MeV)

The explanation for this very peculiar situation lies on experimental reasons connected to the nature of available photon sources. It is only very recently that well-defined energy photon beams with sufficient flux have become available allowing the study of inclusive reactions in the intermediate energy region. I will start by analyzing the problems involved in measuring photo-pion reactions and try to outline what are the future prospects. I will then turn to describe quickly from an experimentalist point of view the motivations and the theoretical frame in which the experiments have been so far discussed ; I will point out some difficulties encountered in these models and leave to more authorized speakers to deal with the perspectives in the field. I will finish by presenting a few recent experiments performed at the Saclay linac which in my sense are significant first steps in the direction of future work on the 100 % duty-cycle facilities available in the forthcoming years.

2. Experimental techniques

2.1 Photon sources

Photons are produced by electrons or positrons in radiative processes yielding continuous spectra. There are two crucial problems in measuring photon induced reactions.

- i) the determination of the energy of the photon
- ii) the monitoring of the photon flux.

Experimental techniques of photo-pion cross section measurements are essentially defined with reference to the photon energy determination problem.

2.2.1 Bremsstrahlung

With a continuous Bremsstrahlung spectrum produced by electrons of energy E_0 (or the virtual photon spectrum from single arm electroproduction) one measures a yield which is the convolution of the photon spectrum with the cross section and the particle detection efficiency :

$$Y(E_0) = \int_{E_{\min}}^{E_{\max}} dE_{\gamma} \frac{dN_{\gamma}}{dE_{\gamma}} (E_{\gamma}, E_0) \frac{d\sigma}{d\Omega} \epsilon$$

The range of useful photons extends from a minimal energy E_{\min} to a maximal energy E_{\max} . This range can be restricted in various ways :

- i) in some exclusive processes the photon energy can be established by a complete kinematical determination of the reaction final state.

For instance in single pion photoproduction off deuterium



measurement of the momentum and angle of two of the final state particles determines the photon energy. However in order to prevent contributions from double pion production one should not allow in the incident beam photons with energy exceeding the useful photon energy by more than the pion rest mass. This is obtained by using an electron beam energy lower than this limit.

- ii) thresholds in the cross section or the detection efficiency can also restrict the range of useful photons.

Pion photoproduction near threshold can be studied by measuring the pion yield as a function of the end-point energy of a Bremsstrahlung spectrum. Since the shape of the cross section variation with energy is known, one gets the magnitude of the cross section from the yield provided that photon spectrum and pion detection efficiency are known.

Another example is neutral pion photoproduction in the Δ region as measured by Booth et al.⁴). Here E_{\min} is determined by the π^0 detector energy threshold set by imposing the opening angle of the two decay photons. The useful photons are restricted to the top 15 MeV of the Bremsstrahlung spectrum.

2.1.2 Photon difference methods

More desirably one monochromatizes the photon beam. Two techniques are used : photon difference method or photon tagging. The latter is by far superior with all respects except high flux ; this only reason explains why the former is still in use.

In the photon difference method one performs two measurements with two photon spectra which differ from each other only in the tip region. The yields difference is thus attributed to the contribution of the photon spectrum difference which is usually restricted to a few MeV below the end point. Electron Bremsstrahlung for two different beam energies has been mostly used.

When positrons are available one obtains quasi-monochromatic in-flight annihilation photons by sending alternatively positrons and electrons on a low Z radiation target, or by using with the positrons a low Z and a high Z radiation target. In each one of these cases by subtracting the two yields one is left with approximately only the contribution of the annihilation. Because of the annihilation peak, this method is more advantageous than the Bremsstrahlung difference as far as signal to noise ratio is concerned. On the other hand positron intensities are lower than electron ones.

The major drawback of difference methods is the difficulty encountered in the study of high excitations in inclusive reactions. Since the photons producing these high excitation states are in much larger number than the useful photons, one has to perform a difference of two big numbers in order to get the contribution of the photon difference spectrum thus producing large statistical uncertainties. This is exemplified in fig. 4 in the case of π^+ inclusive spectra measured on deuterium at backward angle⁵).

In all methods we have so far described, photon normalization requires a knowledge of the photon spectrum shape. In principle a detailed experimental knowledge of the photon spectrum can be obtained by using a pair spectrometer but due to the low duty cycle of existing accelerators, it has very rarely been performed. One usually relies on theoretical spectrum shapes and electron integrated charge measurement (Faraday cup) or integrated photon energy flux measurement (Wilson quantameter). Systematic errors up to 5 % can result from theoretical uncertainties.

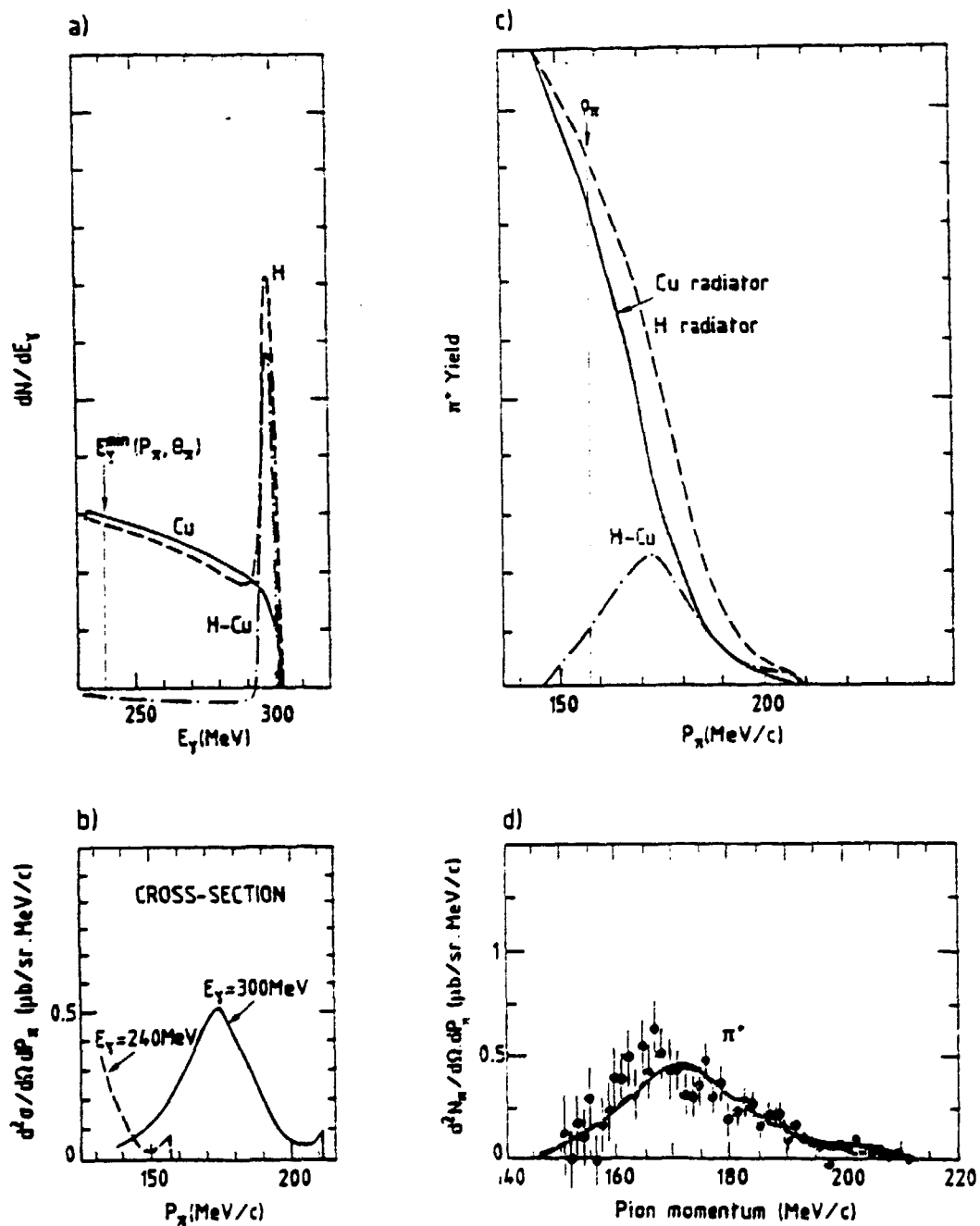


Fig. 4 - The quasi-monochromatic annihilation photons method. a) The photon spectra corresponding to the H and Cu radiation targets and the photon difference spectrum. b) The theoretical π^+ photoproduction differential cross section at $\theta=103.5^\circ$. c) The calculated yields corresponding to the H and Cu radiation targets and the yields difference. d) The experimental data compared to the theoretical yields difference.

2.1.3 Photon tagging

Photon tagging solves both problems of energy determination and photon counting at once (fig. 54), but at the expense of the flux. The photon is tagged by the detection of a particle emitted during the radiation process. This associated particle can be an electron in the case of Bremsstrahlung (or Compton laser backscattering) or a photon in the case of annihilation; it gives information on the photon energy and on its time of creation. A coincidence with a reaction product detector will indicate that the process was initiated by a photon of defined energy. A coincidence with a high efficiency photon detector will count the tagged photon rate. The maximum useful flux of photons is limited by the random coincidence rate between the tagging and the reaction detectors; therefore it is proportional to the ratio of the duty cycle by the tagging coincidence resolving time. For a 10 ns coincidence width and a ratio of true vs. accidental coincidences equal to 1 the number of photons is limited to 10^8 s^{-1} for a 100 % duty-cycle beam.

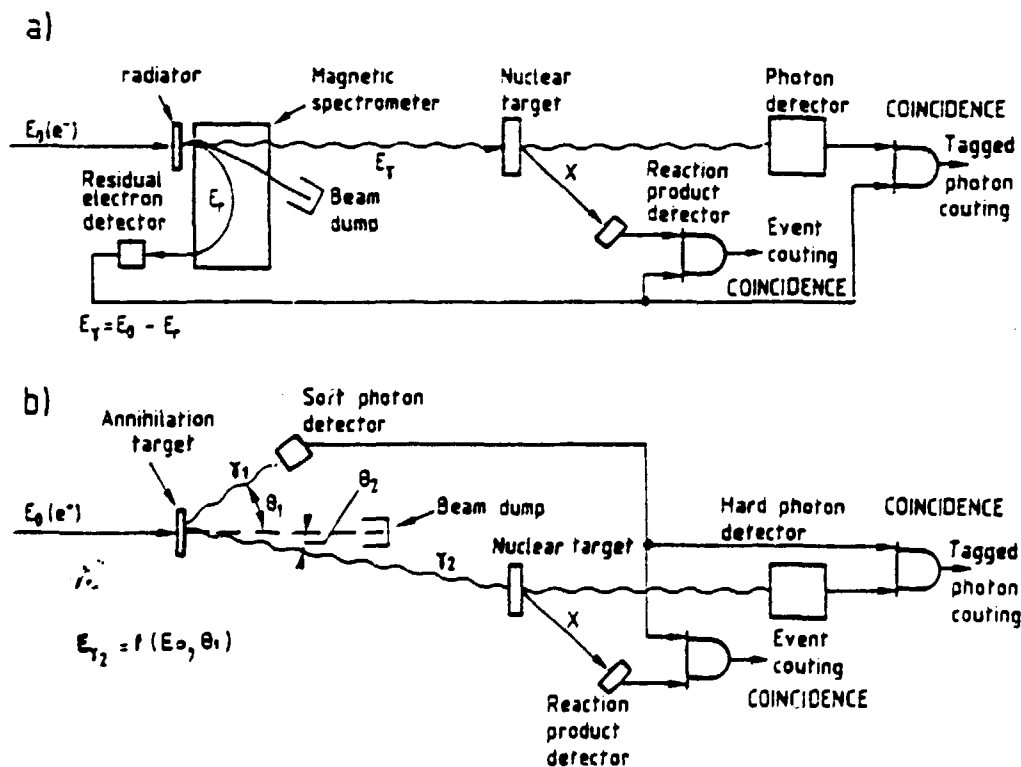


Fig. 5 - Bremsstrahlung and annihilation photon tagging.

In the case of Bremsstrahlung tagging, data can be obtained simultaneously for a large range of photon energies depending on the tagging detector momentum acceptance. For annihilation tagging, the photon energy range is limited by the photon acceptance angle due to the two-body kinematics, and is more adapted for investigation of narrow structures.

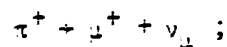
2.2 Pion detection

2.2.1 Charged pions

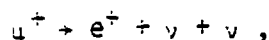
2.2.1.1 Near threshold

Pions of 10 MeV kinetic energy have a 0.6 g/cm^2 range, less than 3 mm path in graphite. The slowing down process is much shorter than the 26 ns mean life.

Positive pions in most targets will stop and decay according to :



muons have a 4.1 MeV energy, their range is 0.15 g/cm^2 less than 1 mm in graphite ; they decay by :



with a mean life of 2.2 μs ; the positron energy spectrum extends up to 53 MeV. The positrons are detected in Cerenkov counters. Note that all angular direction information is lost so that one measures in this way only total cross sections⁶).

Negative pions will make a transition to an atomic orbit when they reach the 1 eV energy region, then cascade down to orbits from which they will get captured by the nucleus. Stopped pion capture takes place preferentially on neutron proton pairs giving rise to neutron pairs. In a deuterium target the $\pi^- + d \rightarrow n + n$ reaction which has a branching ratio of 75 %, has been used⁷) to measure low energy pions by detecting the 70 MeV neutrons at backward angle in a region where the maximum energy for single neutron photoproduction is lower. As for positive pions, angular direction information on the pion is lost.

2.2.1.2 Higher energies

Pion magnetic spectrometers have been devised to detect low and medium energy pions. Owing to the smallness of the cross sections they should combine a large solid angle and because of pion decay a short flight path (50 % of 50 MeV pion decay in a 4 m flight path). Detectors allowing discrimination between electrons and pions may be useful at forward angles where most of the electromagnetic showers are emitted. Decay muons are mistaken for pions, they come mostly from the region between the exit polar face and the detectors ; for low energy pions they can induce large corrections which must be estimated by Monte-Carlo simulations.

2.2.2 Neutral pions

The two gamma decay of the neutral pion is instantaneous (0.34×10^{-16} s mean lifetime at rest). The π^0 are usually detected through their decay photons in lead glass total absorption Cerenkov counters. The Cerenkov light output is directly proportional to the incident pion energy. Veto counters in front of the lead glass blocks allow charged particles rejection. Position sensitive detectors permit localization of the photons and subsequent determination of the pion emission angle. For two nearly equal photon energies a good measurement of the opening angle yields a good measurement of the pion energy. Angular resolution increases dramatically at low energies. Typical characteristics of the LAMPF neutral pion spectrometer³⁾ are 6 MeV energy resolution and $\pm 1^\circ$ angular uncertainty at 150 MeV pion kinetic energy.

3. The theoretical frame of interpretation

The most popular theoretical model of photoproduction is the distorted wave impulse approximation (DWIA) [ref. 9)]. The amplitude for the nucleus is taken equal to the sum of the amplitudes for the nucleons and the only nuclear medium effect is the distortion of the pion wave by the residual nucleus. The amplitude of photoproduction on the individual nucleons is taken to be the amplitude on the free nucleon; the Blomqvist-Laget¹⁰⁾ amplitude is the most convenient one for the nuclear case since it is valid in any reference frame; it contains in addition to the Born terms a phenomenological Δ contribution which has the net effect of changing the magnitude of the nucleon magnetic momentum as a function of energy. The nuclear amplitude for transition from initial nuclear state $\psi_i(J_i, M_i)$ to final state $\psi_f(J_f, M_f)$ and photon polarization state λ reads

$$\sum_{\lambda M_i M_f} \int d^3\vec{r} \psi_f^*(\vec{r}) \psi^{(-)*}(\vec{r}) (\vec{J}_i \cdot \vec{e}_\lambda) \vec{r} e^{i\vec{k} \cdot \vec{r}} \psi_i(\vec{r})$$

$(\vec{J}_i \cdot \vec{e}_\lambda) \vec{r}$ is the elementary amplitude, $\psi^{(-)}$ is the pion wave distorted by its strong interaction with the residual nucleus. Usually it is the solution of the Klein-Gordon equation with the pion nucleus optical potential.

The strategy of pion photoproduction measurements is to study cases in which two of the three ingredients of the model are known in order to isolate the influence of the third one. For instance in charged pion photoproduction at threshold, the elementary amplitude reduces to $E_0 + (\vec{\sigma} \cdot \vec{z}) \tau(\frac{z}{2})$, strong interaction pion distortion is small and can be calculated: one learns about spin-flip transition form factors at momentum transfer of the pion mass; since pion photoproduction is almost not affected by mesonic exchange currents it is a valuable information which must be confronted to the electron magnetic scattering data.

Let us quote a few difficulties with DWIA:

i) off-shell or on-shell prescription for the nucleon on which photoproduction takes place makes large differences in the amplitude value.

ii) to preserve the non-locality of the Blomqvist-Laget operator (due to the propagation of π, N, Δ) one must express all wave functions and carry the integrations required by Fermi motion in the momentum space.

iii) in principle pion distorsion takes place because of rescattering on all nucleons except the one on which photoproduction took place since we are using effective elementary amplitudes ; consequently one is not entitled to use optical potentials which account for pionic atoms and low energy pion elastic scattering data on the initial nucleus ; this remark can be very important for light nuclei.

iv) rescattering effects including charge-exchange processes should be taken into account and it is not clear whether they are not already partially present in the optical potential treatment.

More ambitious and ideally more satisfying is the isobar-hole model¹¹). It gives a unified description of π and γ reactions for Δ dominated processes. Medium modifications are included consistently in both production and final state interaction. The photon excites a Δ hole doorway state which propagates and eventually decays by emission of a pion. Δ properties in the nuclear medium are strongly modified (coupling to the pion annihilation channel, Pauli blocking...). Because of the large contribution of Born terms in charged photoproduction this model has been so far only applied to π^0 coherent photoproduction away from threshold.

4. A few selected pion photoproduction experiments

We will now discuss a few significant experiments which shed light on various aspects of pion photoproduction : reaction mechanism, elementary amplitude on the nucleon, nuclear structure, pion distorsion. The selection of these experiments is strongly biased because of the speaker prejudice.

4.1 Coherent neutral pion photoproduction on nuclei

Neutral pion photoproduction on nuclei near threshold gives information on the coherent reaction mechanism which is dominant in this energy region. The non spin-flip production amplitudes on all nucleons add coherently providing a large enhancement of the cross section. In the case of a spin zero nucleus as ^{12}C , only p-wave production can take place in the elastic process since $0 \rightarrow 0$ electromagnetic transitions with real photons are forbidden. The total $^{12}\text{C}(\gamma, \pi^0)$ cross section has been recently measured¹²) in the 0-50 MeV region above threshold. The experiment was carried out at the Saclay Linac using the tagged photon beam¹³) obtained from in-flight annihilation of e^+ on a LiH target (fig. 6). The tagging detector consisted in a array of 16 multi-wire proportional

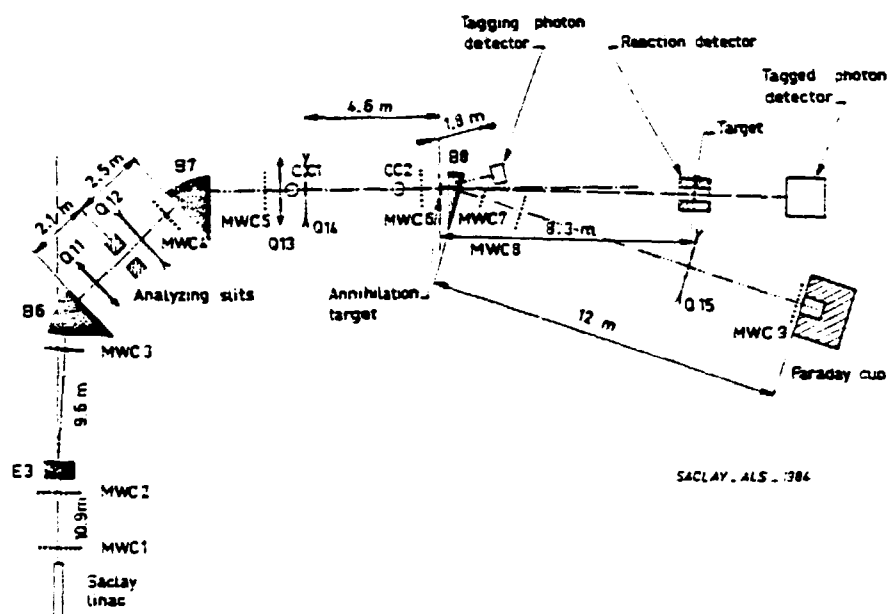


Fig. 6 - The Saclay in-flight positron annihilation tagging installation

chambers, each of them being equipped with a lead converter and a scintillation counter for fast timing coincidences. Typical photon flux at 150 MeV was 10 000 photons per second in a 8 MeV energy range ; photon energy resolution was around 1 MeV FWHM. The two photons from the π^0 decay were observed in coincidence in a $0.8 \times 4\pi$ set of twelve 18 cm thick lead-glass Cerenkov counters (fig. 7). Plastic scintillator veto counters were used to reject electrons originating from showers induced by the primary photon beam in the target. Small contributions of π^0 produced on the protons of the active CH target and of π^0 events associated to proton-decaying levels of ^{12}C , were eliminated off-line.

Results of the cross section measurements are presented in fig. 8. Overall accuracy of the data points is approximately $\pm 5\%$. Experimental values are 80 % larger than those of a previous Bonn measurement¹⁴). In a theoretical calculation S. Boffi and R. Mirando¹⁵) obtain a 70 % enhancement of the plane-wave cross section by including the pion final-state interaction through an optical potential treatment using the Stricker, McIlanus and Carr¹⁶) potential. One can look at near-threshold pion photoproduction as a testing ground for pion nucleus optical potential in a pion energy region intermediary between pionic atoms and low energy pion elastic scattering (pion kinetic energy > 30 MeV), which cannot be reached otherwise. In the case of neutral pion production the model is checked for a different isospin state without Coulomb contribution. Moreover in the elastic process one selects the p-wave part of the potential.

A calculation by Laget using a more complete operator gives nearly the same prediction for the plane wave impulse approximation. However

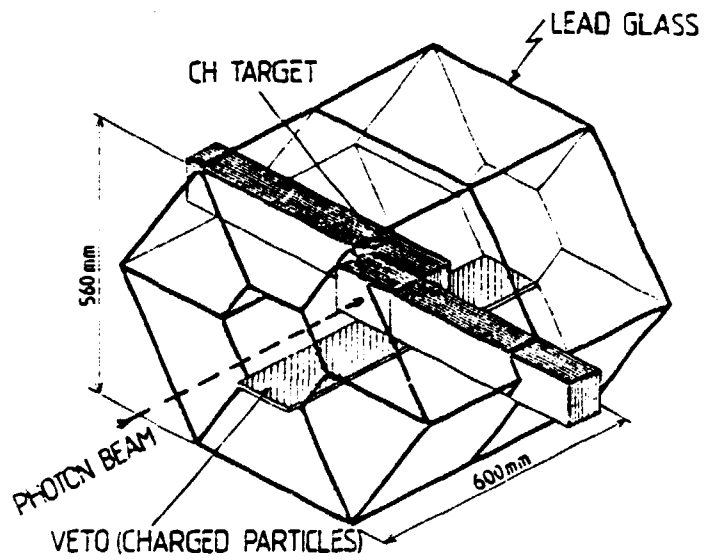


Fig. 7 - The π^0 detector used in the near-threshold photoproduction measurements.

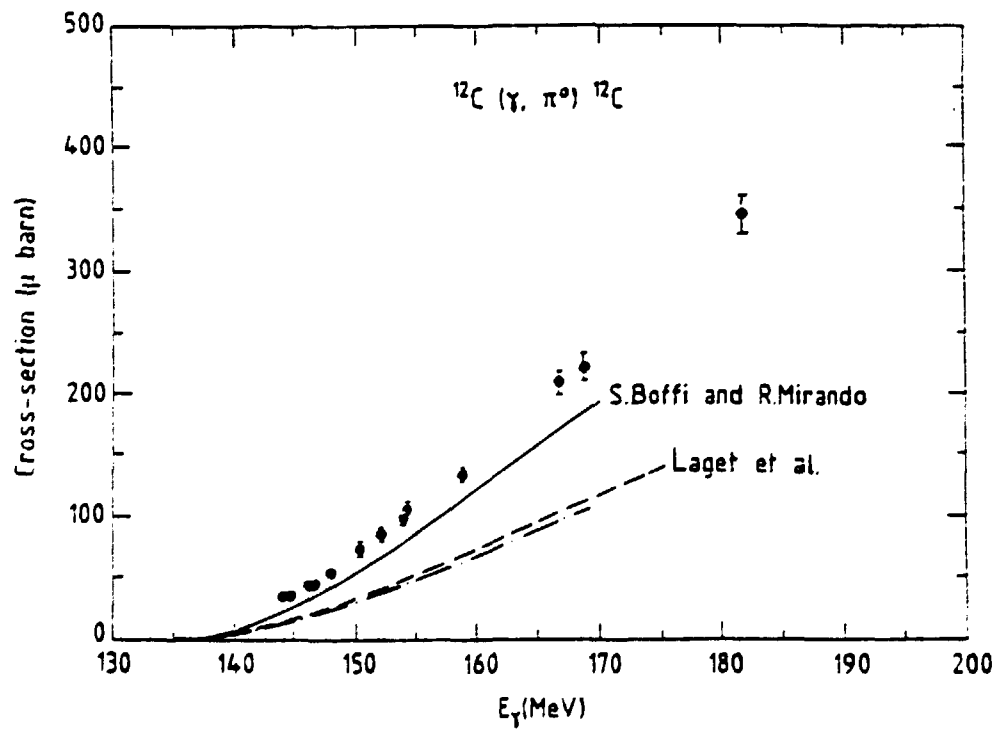


Fig. 8 - The π^0 elastic photoproduction cross section on ^{12}C [ref. 12)]. Dashed and solid curves are respectively PWIA and DWIA from ref. 15). Dash-dotted curve is Laget PWIA calculation.

rescattering corrections should be evaluated before any conclusion is drawn. An experiment is in progress now to study the effect on a few other zero-spin nuclei.

Unfortunately no calculation using the isobar-hole model is available in this energy range. A very interesting measurement has been performed at Bates by Booth et al.¹⁷⁾ in a difficult experiment which measured differential cross section for the same process in ${}^4\text{He}$ at 290 MeV photon energy. The good energy resolution of the π^0 spectrometer was instrumental to the separation of the elastic reaction. The excellent agreement of the cross section size with the isobar-hole model prediction is impressive. More work on carbon is presently in progress at higher energies than those explored in the Saclay experiment (fig. 9).

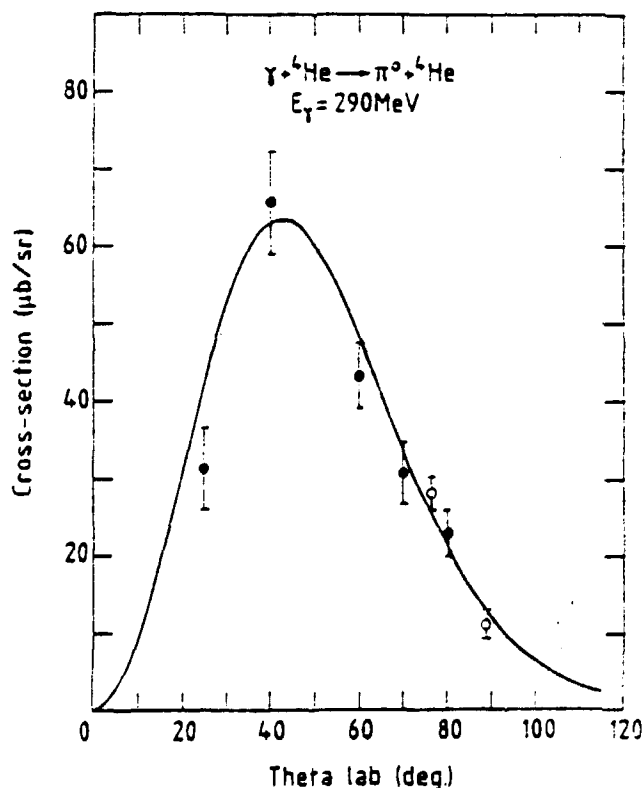


Fig. 9 - The π^0 elastic photoproduction differential cross section on ${}^4\text{He}$ [ref.17)].

4.2 Charged pion photoproduction on deuterium in the resonance region

Few body nuclei are especially well suited for reaction mechanisms studies because realistic wave-functions describing these systems are available and because the number of degrees of freedom is small enough to allow for a multiple scattering treatment of the pion-nucleon and nucleon-nucleon final state interactions. Usually the multiple scattering series converges rapidly and processes up to order 2 are sufficient

to account for the data. Various diagrams illustrating these rescattering processes are shown in fig. 10.

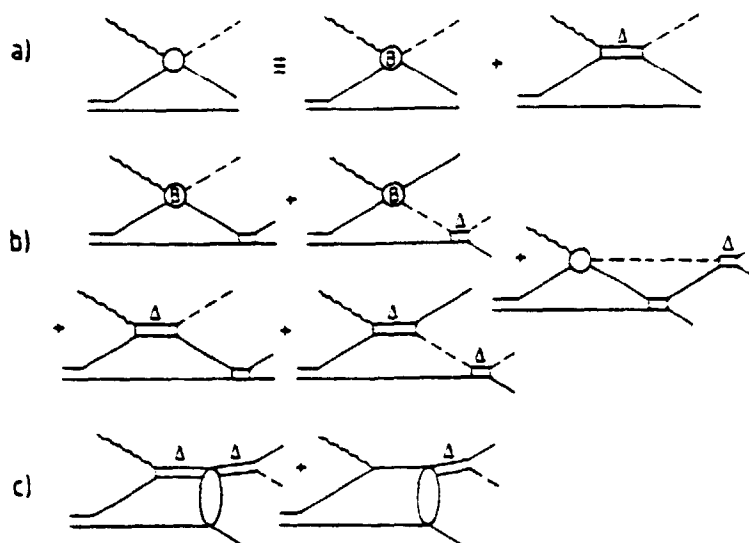


Fig. 10 - Pion photoproduction on deuterium mechanisms.

Single arm experiments emphasize the quasi-free photoproduction mechanism on the individual nucleons. In fig. 11 we display π^+ and π^- spectra obtained with a 300 MrV photon annihilation quasi-monochromatic beam at 46.4° [ref. 5]). The broadening and the energy shift of the quasi-free peak from the pion production line on the nucleon result from the Fermi motion and the binding energy of the nucleons. Pion rescattering corrections are small throughout the spectra. Final state strong attraction of the two nucleons when their relative energy is small produce an enhancement at the high momentum tip of the spectra. The data show good agreement with a calculation by Laget which includes the first order rescattering processes. Such experiments are important because they give an overall constraint on the models in a region where one-body processes are dominant ; they constitute a necessary stage before looking into deviations to one-body processes.

The strategy of double arm coincidence experiments consists in the selection of kinematical conditions which minimize the contribution of quasi-free photoproduction in order to emphasize specific many-body effects. For single photoproduction on nuclei, one needs monochromatic photons to define completely the three-body final state kinematics by the detection of two particles in coincidence. However in the case of deuterium the nature of the undetected particle is known and one can use instead Bremsstrahlung photons without bringing any ambiguity. This is a definite advantage which compensates for the smallness of the detectors acceptances and also the low duty-cycle beam which were used in this experiment.

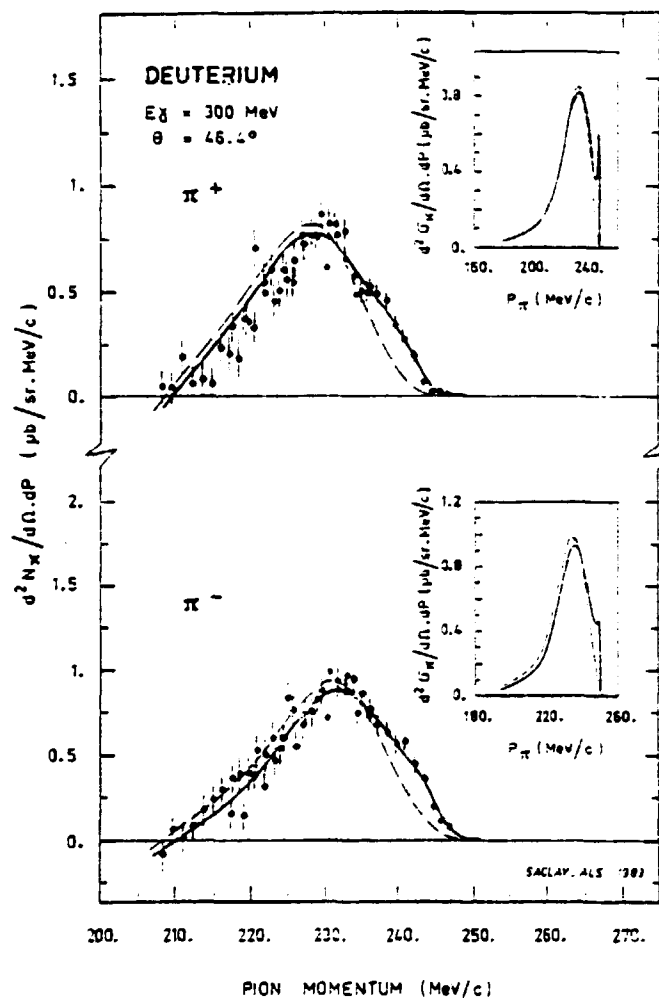
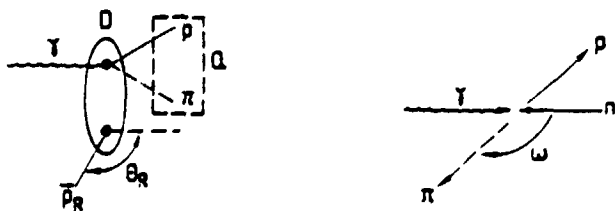


Fig. 11 - π^+ and π^- photoproduction spectra on deuterium at $E_\gamma = 300$ MeV and $\theta = 46.4^\circ$. Dashed line curve is the prediction for quasi-free production; solid line curve includes nucleon-nucleon rescattering. The corresponding doubly differential cross sections are shown in the insets.



Pion nucleon c.m. frame

Fig. 12 - Schematic representation of the quasi-free pion photoproduction on deuterium.

The principle of the measurements¹⁸⁾ carried out at the Saclay Linac eight years ago is sketched in fig. 12. The modulus P_R of the spectator nucleon momentum and the kinematics of the photoproduction process on the other nucleon (photon nucleon invariant mass $Q_{N\pi}$, and photoproduction angle ω of the two-body system in the center of mass referential) are kept constant while the spectator nucleon angle θ_R is varied. Depending on the angles and momenta of the three particles one can perform either a $d(\gamma, p\pi^-)p$ or a $d(\gamma, pp)\pi^-$ experiment. For quasi-free photoproduction one expects the angular distribution obtained when θ_R is varied, to be flat (fig. 13). Indeed this is observed to be true for low

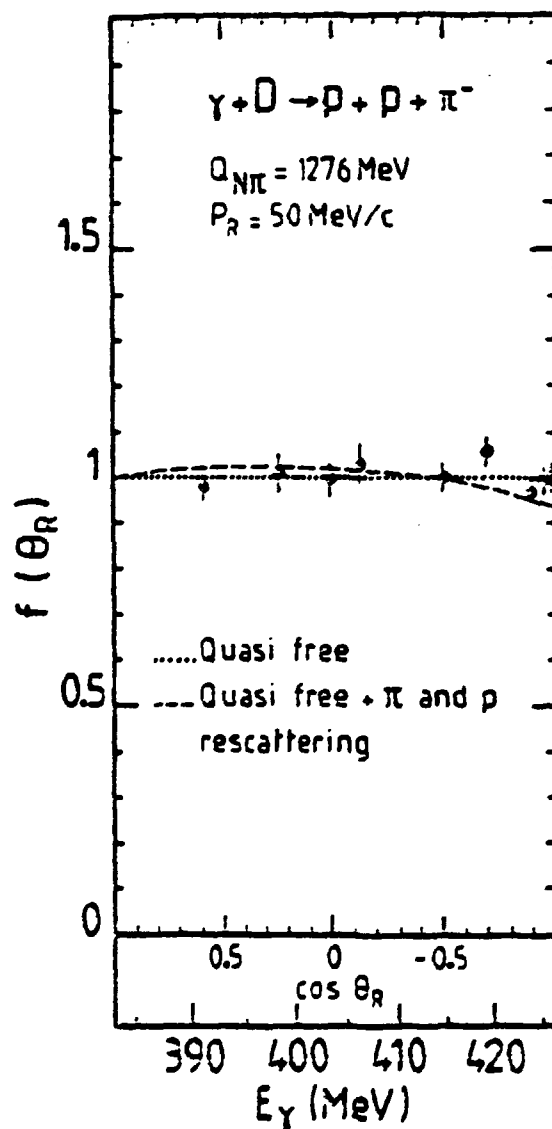


Fig. 13 - The ratio of the measured yield of the reaction $d(\gamma, p\pi^-)p$ to the calculated quasi-free photoproduction yield as a function of $\cos\theta_R$
 $P_R = 50 \text{ MeV}/c$.

values of P_R ($P_R = 50$ MeV/c). Conversely for large values of P_R ($P_R > 150$ MeV/c) the angular distribution shows sizable deviations from the quasi-free (fig. 14).

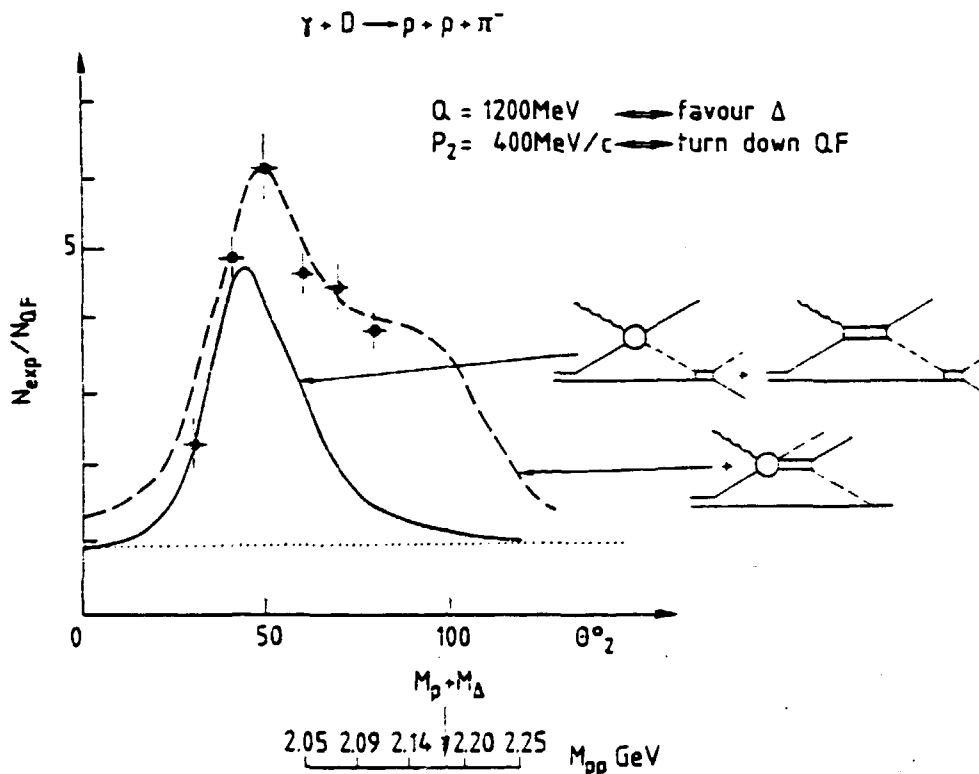


Fig. 14 - The same as fig. 13 for $P_R = 400$ MeV/c.

A systematic exploration of the three-body state system πNN would require higher energy and higher duty-cycle machines associated with larger solid angle and acceptance detectors than those presently available. Also an extension of these experiments to nuclear systems more bound than deuterium would be desirable since higher nuclear density would enhance the many-body effects. This would necessitate very performing tagged photons installations on high duty-cycle accelerators associated to 4π detectors.

References

- 1) G. Audit et al., Contributed paper D23, Nuclear Physics with Electr. Probes, Paris (1985).
- 2) G. Audit et al., private communication.
- 3) K. Shoda et al., preprint (1984).
- 4) D.R. Tiegner et al., Phys. Rev. Lett. 53 (1984) 755.
- 5) J.-L. Faure et al., Nucl. Phys. A424 (1984) 383.
- 6) G. Audit et al., Phys. Rev. C15 (1977) 1415.
- 7) F. Klein et al., Nucl. Instr. Meth. 180 (1981) 185.

- 8) H.W. Baer et al., Nucl. Instr. Meth. 180 (1981) 445.
- 9) K.M. Singham and F. Tabakin, Ann. of Phys. 135 (1981) 71.
- 10) I. Blomqvist and J.-M. Laget, Nucl. Phys. A280 (1977) 405.
- 11) J.H. Koch and E.J. Moniz, Phys. Rev. C27 (1983) 751.
- 12) P.E. Argan et al., Contributed paper Es, Nuclear Physics with Electr. Probes, Paris (1985).
- 13) P. Argan et al., Nucl. Instr. Meth. 228 (1984) 20.
- 14) J. Arends et al., Z. Phys. A311 (1983) 367.
- 15) S. Boffi and R. Miranda, preprint (1985).
- 16) K. Stricker, H. McManus and J.A. Carr, Phys. Rev. C19 (1979) 929.
- 17) E.C. Booth et al., Bates Linear Accelerator Center, Annual report (1984).
- 18) P.E. Argan et al., Phys. Rev. Lett. 41 (1978) 86.